NONLINEAR WAVE PROPAGATION IN PHOTONIC CRYSTAL FIBERS

Haider Ali Muse
Department of Physical Foundations of Electronic Engineering
Kharkiv national university of radio electronics
Kharkiv, Ukraine
hadr_2005@yahoo.com

Yuri Machehin
Department of Physical Foundations of Electronic Engineering
Kharkiv national university of radio electronics
Kharkiv, Ukraine

Abstract
Wave propagation is a fundamental phenomenon occurring in several physical systems. The spectra have been used by others to develop optical frequency standards. The process can potentially be used for frequency conversion in fiber optic network. In this system the dispersive properties can be controlled by the optical lattice making it possible to achieve phase-matched four wave mixing, like look the process taking place in the photonic crystal fibers (PCFs). In this paper will focus on two such systems the propagation nonlinear wave in photonic crystal fibers and the propagation of matter waves in optical lattices.
Keywords: photonic crystal fibers; nonlinear optics, propagation, photonic crystal fibers, Maxwells

1. Introduction

Photonic crystals (PhCs) These materials have highly periodic structures that can be designed to control and manipulate the propagation of light. Electromagnetic wave propagation in periodic media was first studied by Lord Rayleigh in 1888 [1]. These structures were one-dimensional (PhCs) which have a narrow band gap prohibiting light propagation through the planes. About 100 years later, in 1987, Yablonovitch and John - by using the tools of classical electromagnetism and solid-state physics - introduced the concepts of omnidirectional photonic bandgaps in two and three dimensions [2, 3]. From then, the name "photonic crystal" was created and led to many subsequent developments in their fabrication, theory, and application. A few years later in 1991, Yablonovitch and co-workers produced the first (PhCs) by mechanically drilling holes a millimeter in diameter into a block of material with a refractive index of 3.6 [4]. Other structures, which have band gaps at microwave and radio frequencies, are being used to make e.g antennas that direct radiation away from the heads of mobile phone users. There are typically three types of computational methods: time-domain "numerical experiments" [5–10] that model the time-evolution of the fields with arbitrary starting conditions in a discredited system (e.g. using finite differences); definite-frequency transfer matrices [11–14] wherein the scattering matrices are computed to extract transmission/reflection through the structure; and frequency-domain methods [15] to directly extract the Bloch fields and frequencies by diagonalizing the eigenoperator. The first two categories intuitively correspond to directly measurable quantities such as transmission, whereas the third is more abstract, yielding the band diagrams that provides a guide to interpretation of measurements as well as a starting-point for device design and semi-analytical methods. Maxwell's equations can be solved numerically either in the time domain or in the frequency domain. Each method has its strong points and its disadvantages. The frequency domain method, which assumes that the time dependence is harmonic, plays an important role in calculating the eigenstates and band structures. On the other hand, the time domain method, which solves the time dependent Maxwell equations directly on spatial grids, is well suited for computing problems that involve the evolution of electromagnetic fields and for systems containing complex materials. The computational method we used to simulate (PhCs) structures is the time domain method. The

simulation is based on the well known finite-difference time domain (FDTD) technique. The FDTD method is a rigorous solution to Maxwell's equation and does not have any approximations or theoretical restrictions. This method is widely used as a propagation solution technique in integrated optics. FDTD is a direct solution of Maxwell's curl equations and therefore includes many more effects than a solution of the monochromatic wave equation. About a decade later on, one has successfully fabricated (PhCs) that work in the near-infrared (780-3000 nm) and in the visible (450-750 nm) regions of the spectrum.

2. The objective of the paper

- These fibers are based on a new and very promising technology and could provide solutions to many optical problems in telecommunications, light source manufacturing and has already revolutionized the field of frequency metrology. The light itself can also provide periodic structuring through an optical lattice and in this system matter wave propagation will be investigated.
- In telecommunication the fibers could provide many new solutions. The PBG fibers offer the possibility of low losses and dispersion, a possible competitor to conventional fibers.
- The theoretical modelling of light propagation in the PCFs is needed, to get a good understanding of the processes taking place in supercontinuum generation, and to give input to the design and development of new fiber structures and applications.

3. Photonic crystal (PhCs)

Photonic crystals (PhCs) are inhomogeneous dielectric media with periodic variation of the refractive index. In general, (PhCs) have a photonic band gap. That is the range of frequencies in which light cannot propagate through the structure. (PhCs) are optical media with spatially periodic properties. This definition is too general to be useful in all contexts, and there has been some debate about the conditions under which it is legitimate to use the term [16]. (PhCs) are periodic structures of dielectric materials and can today be produced with almost any imaginable structure. It is only a decade ago that Bose-Einstein condensation was first achieved in alkali gases [17, 18] and it has certainly turned into a very rich field since the condensates are very flexible model systems for solid state physics and statistical physics in general. The dynamics of the wave propagation in both systems is mainly determined by the interplay between dispersive and nonlinear effects. In the Bose-Einstein condensates (BECs) the nonlinear response originates in the s-wave scattering between atom pairs, whereas the nonlinearity in the PCFs stems from saturation and optical pumping accounted for through a nonlinear susceptibility. The micro-structuring of the PCFs leads to unique and tailorable dispersive properties. In the Bose-Einstein condensed system the optical lattice does the job of tuning the dispersion.

4. Photonic crystal fibres (PCFs)

Photonic-crystal fibres (PCFs) [19, 20], also referred to as microstructure, or holey, fibres, are optical waveguides of a new type. In PCFs, radiation can be transmitted through either a solid (**Fig. 1, a–d**) or hollow (**Fig. 2, b**) core, surrounded with a microstructured cladding, consisting of an array of cylindrical air holes running along the fibre axis. Such a microstructure is usually fabricated by drawing a perform composed of capillary tubes and solid silica rods.

Along with conventional waveguide regimes, provided by total internal reflection, PCFs under certain conditions can support guided modes of electromagnetic radiation due to the high reflectivity of their cladding within photonic band-gaps (PBGs) or regions of low densities of photonic states [21, 22], as well as by the antiresonance mechanism of waveguiding [20, 23]. Such regimes can be supported by fibres with a hollow [22, 24, 25] or solid [26] core and a two-dimensionally periodic (photonic crystal) cladding. A high reflectivity provided by the PBGs in the transmission of such a cladding confines radiation in a hollow core, substantially reducing the loss, which is typical of hollow-core-guided modes in conventional, capillary-type hollow waveguides and which rapidly grow with a decrease in the diameter of the hollow core [27, 28]. Unique properties of PCFs open up new routes for a long-distance transmission of electromagnetic radiation [19, 20], as well as for nonlinear-optical transformation of laser pulses [29]. As shown by Knight et al. [30], PCFs can support single-mode waveguiding within a remarkably broad frequency range. Photonic-crystal fibres offer new solutions for laser physics, nonlinear optics, and optical technologies, as they combine dispersion tuneability and a high degree of light-field confinement in the fibre core. Dispersion of such fibres is tailored by changing their core–cladding

geometry [31, 32], while a strong light-field confinement is achieved due to the high refractive-index step between the core and the microstructure cladding [33]. Controlled dispersion of PCFs is the key to new solutions in optical telecommunications and ultrafast photonics. The high degree of light-field confinement, on the other hand, radically enhances the whole catalogue of nonlinear-optical processes and allows observation of new nonlinear-optical phenomena. **Fig. 1, a, b** display the cross-section views of PCFs with a high refractive-index step from the fibre core to the fibre cladding, controlled by the air-filling fraction of the microstructure cladding.

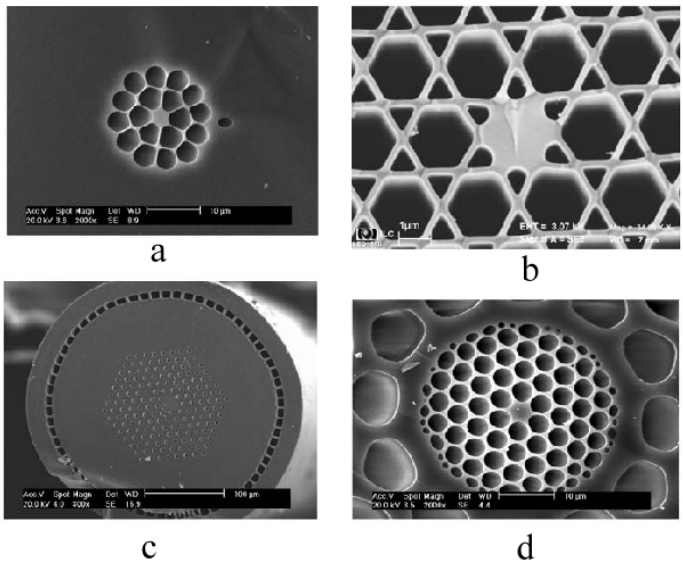

Fig. 1. Cross-section images of photonic-crystal fibres: (**a**–**c**) fibres with a high optical nonlinearity provided by a small fibre core and a high refractive-index contrast between the core and the cladding, (**d**) dual-cladding PCF

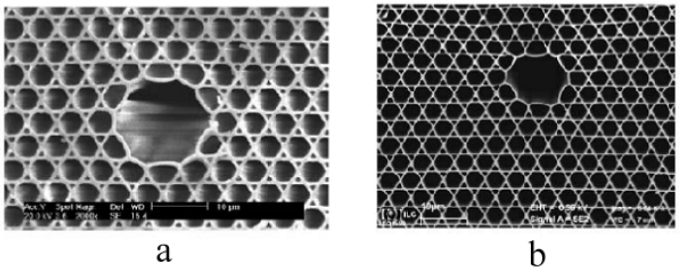

Fig. 2 Cross-section of photonic-crystal fibres : (**a**) large-mode-area PCF, and (**b**) hollow-core PCFs

The fibres of this type can strongly confine the electromagnetic field in the fibre core, providing high optical nonlinearities, thus radically enhancing nonlinearoptical interactions of light fields. Highly efficient fibre-format frequency converters of ultrashort light pulses [29] and PCF super-continuum sources [34, 35] based on highly nonlinear PCFs (**Fig. 1, a, b**) are at the heart of advanced systems used in optical metrology [36, 37], ultrafast optical science [38, 39], laser biomedicine [40], nonlinear spectroscopy [41, 42], and nonlinear microscopy [43, 44]. The possibility of dispersion tailoring makes PCFs valuable components for dispersion balance and dispersion compensation in fibre-optic laser oscillators intended to generate ultrashort light pulses with a high quality of temporal envelope. Lim et al. [45] have demonstrated an ytterbium-fibre laser source of 100-fs pulses with an energy of about 1 nJ with dispersion compensation based on a PCF instead of free-space diffraction gratings. A highly birefringent hollow-core PCF [46] provides a robust

polarization-maintaining generation of 70-fs laser pulses with an energy of about 1 nJ in a fibre laser system [47]. Isomäki and Okhotnikov [48] have achieved dispersion balance in an ytterbium femtosecond fibre laser using an all-solid PBG fibre [26]. In contrast to silica–air index-guiding microstructure fibres, including silica and air holes, an all-solid PBG fibre guides light along a silica core surrounded with a two-dimensional periodic lattice of high-index glass inclusions. Dispersion tailoring and a high nonlinearity of small-core PCFs, on the other hand, allow efficient optical parametric oscillation and amplification due to the third-order optical nonlinearity of the fibre material [49, 50]. Optical parametric oscillators based on PCFs can serve as efficient sources of correlated photon pairs [51, 52]. The maximum laser fluence in an optical system is limited by the laser damage of material of optical components. An increase in a fibre cross section is a standard strategy for increasing the energy of laser pulses delivered by fibre lasers. Standard large-core-area fibres are, however, multimode, making it difficult to achieve a high quality of the transverse beam profile. This difficulty can be resolved by using PCFs with small-diameter air holes in the cladding, which filter out high-order waveguide modes [30, 53]. This strategy can provide single-mode waveguiding even for largecore- area fibres [54, 55] (**Fig. 1, c**). A dual-clad PCF design helps to confine the pump field in the microstructured cladding and to optimize a spatial overlap between the pump field and laser radiation. In this type of PCFs, the microstructured part of the fibre is isolated from the cladding by an array of large-diameter air holes (**Fig. 1, c**). Large-mode-area ytterbium-doped PCFs [56, 57] are employed for the creation of high-power lasers [55, 58, 59]. Large-mode-area silica PCFs are also used for the compression of high-power subpicosecond laser pulses [60] and the generation of supercontinuum with an energy in excess of 1 μJ [61, 62]. Photonic-crystal fibre design presented in (**Fig. 1, d**) is of special interest also for the development of novel fibre-optic sensors [63, 64]. In sensors of this type, excitation radiation is delivered to an object along the fibre core. The inner part of the microstructured cladding features micrometer-diameter air holes and serves for a high-numerical-aperture collection of the scattered or fluorescent signal from the object, as well as for the fibre delivery of this signal to a detector. With such a scheme of sensing, a detector can be placed next to a radiation source [65, 64]. This fibre design is advantageous for sensing chemical and biological samples by means of one- and two-photon luminescence. A microstructured cladding of PCF can be also conveniently filled with a liquid-phase analyte. Radiation propagating along the fibre core will then induce luminescence of the analyte, allowing the detection of specific types of molecules from the minimal amount of analyte [64]. Such fibre sensors can be integrated into chemical and biological data libraries and data analyzers, including biochips, suggesting an attractive format for the readout and processing of the data stored in such devices. The energy of laser pulses in fibre-optic devices can be radically increased through the use of hollow-core fibres. For standard, capillary-type fibres, however, the loss rapidly grows (as $\infty a-3$) with a decrease in the core radius a [27, 28]. Because of this problem, such fibres cannot provide single-mode guiding or help to achieve high intensities for pulses with moderate peak powers. The loss of coreguided modes in hollow fibres can be radically reduced if the fibre has a two dimensionally periodic (photonic crystal) cladding [24, 22, 25] (**Fig. 2, a, b**). A strong coupling of incident and reflected waves, occurring within a limited frequency range, called a photonic band-gap, leads to a high reflectivity of a periodically structured cladding, allowing low-loss guiding of light in a hollow fibre core. Hollow PCF compressors in fibre-laser systems [66, 67] allow the generation of output light pulses with a pulse width on the order of 100 fs in the megawatt range of peak powers. Thus, PCFs play the key role in the development of novel fibre-laser sources of ultrashort light pulses and creation of fibre-format components for the control of such pulses. In what follows, we examine the physical mechanisms behind supercontinuum generation in such fibres, analyze various scenarios of spectral broadening and wavelength conversion, and discuss applications of PCF white-light sources and frequency converters in nonlinear spectroscopy and microscopy, as well as in optical metrology.

5. Dispersion properties of (PCFs)

In a homogeneous medium the dispersion relation between wave vector k and frequency ω of the propagating light is given through the refractive index of the material $\omega=c|k|/n$. In a PCF it is the combined effect of the material dispersion and the band structure arising from the 2D photonic crystal that determines the dispersion characteristics of the fiber. For propagation in fibers it is the dispersion for the wave vector component along the z-direction kz that is the interest-

ing parameter. In the fiber optics literature kz is referred to as the propagation constant β. It is then reasonable to define an effective refractive index as

$$n_{eff} = \frac{\beta c}{\omega_{fund}}, \tag{1}$$

where ω_{fund}. denotes the frequencies of the lowest lying mode in the fiber. The higher derivatives of the propagation constant are given as

$$\beta_n(\omega) = \frac{\partial^n \beta}{\partial \omega^n}, \tag{2}$$

and the second order dispersion $D = -\frac{2\pi c}{\lambda^2}\beta_2$ is just another way of expressing β_2. The zero-dispersion wavelength (λ_{ZD}) is defined as the free space wavelength $\lambda = \frac{2\pi c}{\omega}$ where $\beta_2 = 0$.

A cross-section of an index guiding PCF is shown in **Fig. 3, a** calculation of the dispersion properties and effective area of this fiber will be sketched. The dispersion given by $\beta_2(\lambda)$ is shown in **Fig. 3** and the fiber has λ_{ZD} = 721 nm, whereas the zero dispersion wavelength for bulk silica is found around 1300 nm.

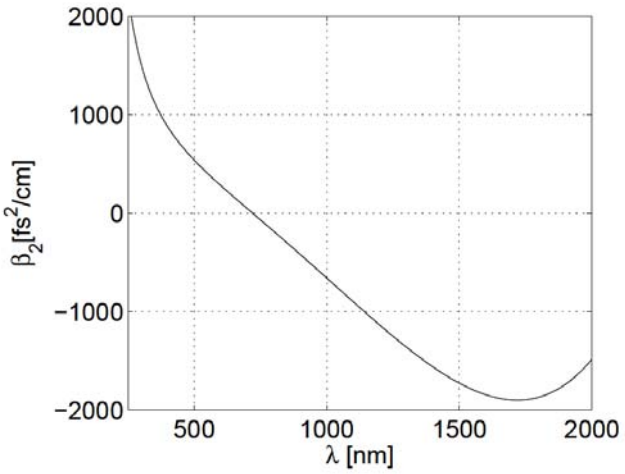

Fig. 3. Dispersion characteristics for the fundamental frequency mode of the 1.7μm core diameter PCF shown in **Fig. 5**

The zero dispersion wavelength for this fiber has consequently been shifted into the visible regime due to the micro-structuring. This widely tunable group velocity dispersion is an extremely valuable property of the PCFs. The dispersion can be tuned by a proper choice of the size of the air holes, the distance between the holes (pitch) and the size of the central defect. A general tendency is that the zero dispersion wavelength is found at a shorter wavelength when the fraction of air filling is increased and the central defect is decreased [68]. It is possible to manufacture fibers with zero dispersion wavelengths between 500 and 1500 nm. Another general trend is that decreasing either the pitch or the hole-size leads to a higher curvature of the dispersion profile, eventually leading to two closely lying zero dispersion wavelengths. The fibers can be made with cores down to 1μm in diameter. Due to the small core areas huge intensities can be obtained in the cores of the fibers. Consequently, such fibers will exhibit a highly nonlinear response. Another very useful property of the fibers is that they can be made endlessly single mode. Only one mode should have a propagation constant between the effective propagation constants for the cladding and the core i.e. $n_{\text{core}}k > \beta > n_{\text{clad}}k$, where k is the free space propagation constant. The restriction corresponds

to only one solution to Maxwell's equations propagating in the core and evanescent in the cladding. The effective frequency parameter is given by [69]

$$V_{eff} = \left(\frac{2\pi\rho}{\lambda}\right)\sqrt{n_{core}^2 - n_{clad}^2}\ , \tag{3}$$

where ρ is the core radius. For the fiber to be single mode Veff should be below 2.405. As λ decreases, the effective index of the cladding n_{clad} increases, because more intensity of the light will be confined to the silica part of the cladding. Consequently, Veff can be kept below 2.405 for a wide range of wavelengths and the fiber is said to be endlessly single mode. In this way fibers, even with a very large core, can be made endlessly single mode [70]. As the mode area of the fiber increases the relative intensity in the core will decrease. Hence the fibers can be used for linear propagation, where a lot of power can be delivered without going into a nonlinear propagation regime.

6. Attenuation properties of (PCFs)

If the transverse scale of a (PCFs) changes without otherwise changing the fibre's structure, the wavelength λ_c of minimum attenuation must scale in proportion [71]. Without recourse to the approximations of the previous section, the mean square amplitude of the roughness component that couples light into modes with effective indices between n and $n+\delta n$ is:

$$u^2 = \frac{k_B T}{4\pi\gamma(n-n_0)}\coth\left(\frac{(n-n_0)kW}{2}\right)\delta n, \tag{4}$$

where γ – the surface tension; k_B – Boltzmann's constant; T – the temperature.

The attenuation to these modes is proportional to u^2 [72] but the only other independent length scale it can vary with is λ_c. As attenuation has units of inverse length, it must therefore by dimensional analysis be inversely proportional to the cube of λ_c. If this is true for every set of destination modes, it must be true for the net attenuation α to all destination modes, so:

$$\alpha(\lambda_c) \approx \frac{1}{\lambda_c^3}. \tag{5}$$

This equation [71], predicts the attenuation of a given fibre drawn to operate at different wavelengths. The result differs from the familiar $1/\lambda^4$ dependence of Rayleigh scattering in bulk media [73], and importantly applies to inhomogeneities at all length scales not just those small compared to λ. The fibres had 7-cell cores but were drawn to different scales, giving them different λ_c but otherwise comparable properties [71]. The minimum attenuation is plotted in **Fig. 4** against λ_c on a log-log scale. A straight-line fit is shown and has a slope of 3.07, supporting the predicted inverse cubic dependence in Eq. (5).

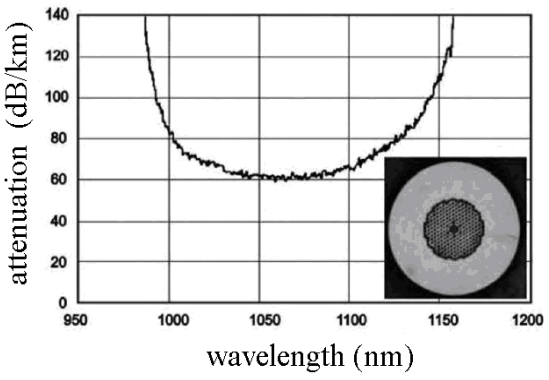

Fig. 4. Attenuation spectrum of a (PCF)

The minimum optical attenuation of ~0.15 dB/km in conventional fibres is determined by fundamental scattering and absorption processes in the high-purity glass [73], leaving little prospect of much improvement. Over 99% of the light in (PCFs) can propagate in air [71] and avoid these loss mechanisms, making (PCFs) promising candidates as future ultra-low loss telecommunication fibres. The lowest loss reported in photonic crystal fibres is 1.7 dB/km [71], though we have since reduced this to 1.2dB/km. Since only a small fraction of the light propagates in silica, the effect ofmaterial nonlinearities is insignificant and the fibers do not suffer from the same limitations on loss as conventional fibers made from solid material alone.

7. Maxwells equations

To get the dispersion characteristics (ω versus β) of the fiber structure Maxwell's equations have to be solved: Decoupling Maxwells equations with no free charges and currents, assuming linear response of the medium and no losses leads to a wave equation for the $H\omega(r)$ field

$$\nabla \times \left[\frac{1}{\varepsilon(r)} \nabla \times H_{\omega}(r) \right] = \left(\frac{\omega}{c} \right)^2 H_{\omega}(r), \tag{6}$$

where ε is the dielectric function. Here the fields have been expanded into a set of harmonic modes $H\omega(r, t) = Re\ (H\omega(r)e^{-i\omega t})$ with frequency ω. This can be done without further loss of generality since Maxwell's equations have already been assumed linear [74, 75]. Because of translational symmetry along the z-axis the dielectric function only depends on (x, y), consequently the harmonic modes can be expressed on the following form:

$$H_{\omega}(r) = \sum_{m} \alpha_m h_m(x, y) e^{-i\beta^{(m)}(\omega) z}, \tag{7}$$

where m denotes the m th eigenmode with transverse part $\boldsymbol{h}m(x, y)$ and propagation constant $\beta^{(m)}(\omega)$. After expanding in a plane wave basis the matrix eigenvalue problem is solved leading to the (fully vectorial) eigenmodes. The method is described in [74, 76]. Johnson and Joannopoulos have developed a freely available code, to solve Maxwell's equations [77]. With this code and a dielectric function based on the image of **Fig. 5.**

Niels Asger Mortensen and Jes Broeng from Crystal Fibre have calculated the transverse part $\boldsymbol{h}m\ (x,y)$ of the eigen modes and propagation constants $\beta^{(m)}(\omega)$ [78] see **Fig. 6**.

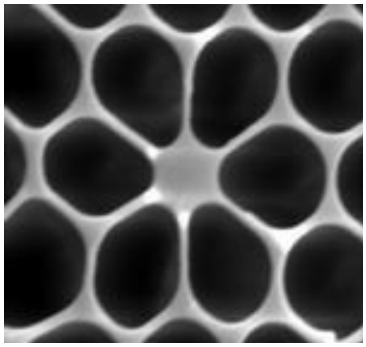

Fig. 5. Image of the end face of a PCF with a core diameter of 1.7μm. Picture provided by Crystal Fibre A/S

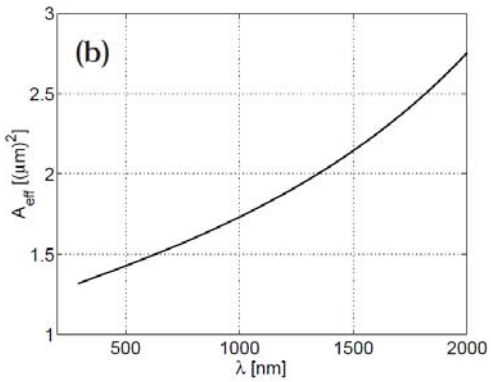

Fig. 6. Effective area of the same fiber. Calculations carried out by Niels Asger Mortensen / Jes Broeng from Crystal Fibre A/S

Both the material dispersion of silica and the dispersion due to the micro-structuring of the fibers contribute to the effective refractive index of the fundamental mode

$$n_{eff} = n_{\text{material}} + n_{\text{eff,bandstructure}} - n_{\text{constant}}, \tag{8}$$

The effective propagation constant β of the fundamental mode can subsequently be found from Eq. (1) by inserting *n*eff. The refractive index of silica n_{material} has been calculated from the Sellmeier formula

$$n_{material}^2(\lambda) = 1 + \sum_{j=1}^{p} \frac{B_j^2}{1 - \left(\frac{\lambda_j}{\lambda}\right)^2}, \tag{9}$$

where λ_j is an atomic resonance in the fused silica. For the calculations the parameters given in [79] have been used: B_1=0.6961663, B_2=0.4079426, B_3=0.8974794, λ_1=0.0684043μm, λ_2=0.1162414μm, λ_3=9.896161μm. The contribution to the effective refractive index from the micro-structuring $n_{\text{eff,bandstructure,}}$ has been calculated by assuming a frequency independent refractive index of silica (n_{constant}=1.45) in the dielectric function $\varepsilon(x, y)$ in Eq. (6). By solving the equation the propagation constant of the fundamental mode $\beta^{(1)}$ is found, giving $n_{\text{eff, bandstructure}} = c\beta^{(1)}/\omega$. To include the contribution to n_{eff} from silica only once, the constant offset n_{constant} in Eq. (8) is introduced. In fact this constant term will have no impact on the simulations in the following chapters, since a frame of reference moving with the group velocity of the propagating pulse is chosen. Based on a SEM-picture of the fiber end face shown in **Fig. 5** the propagation constant of the shown 1.7μm core diameter PCF has been calculated using the method sketched above. The group velocity dispersion β2, calculated from the propagation constant, is shown on **Fig. 3**. A mode corresponding to the other polarization state exists, but in the calculations presented in the following chapters only propagation in one polarization mode will be considered, even though for example the fiber on Fig.(5) is not polarization maintaining. The frequency dependency of the refractive index of silica can also be taken into account initially through a frequency dependent dielectric function $\varepsilon(x,y,\omega)$. Eq. (6) then has to be solved self consistently. When comparing the two methods no major differences appear. An effective area of a mode in a fiber can be defined as [78, 79]

$$A_{eff,n}(\omega) = \frac{\left[\int dxdy \left|h_n(x,y)\right|^2\right]^2}{\int dxdy \left|h_n(x,y)\right|^4}, \tag{10}$$

where $|\boldsymbol{h}n(x, y)|^2$ is proportional to the intensity distribution in the fiber. **Fig. 6** shows the effective area of the fundamental mode for the 1.7 μm core diameter PCF. It is the high index contrast between silica and air that makes the relatively low effective areas in PCFs possible [78].

8. The nonlinear Schrödinger equation

The simplest form of the nonlinear Schrödinger equation is given by

$$\frac{d}{dz}A = -i\frac{\beta_2}{2}\frac{\partial^2}{\partial t^2}A + i\gamma\left|A\right|^2 A, \tag{11}$$

On the way to the equation above a more general version of the nonlinear Schrödinger equation will be found. The first term describes the second order dispersion determined by the material and the geometrical structure of the fiber as described in the previous chapter. The second term is the nonlinearity, which depends upon the polarizability of the material through $\chi(3)$ and scales with the third power of the electric field. The nonlinear Schrödinger equation has been applied in fiber optics since the beginning of the eighties, where it was used to describe Mollenauer's first experimental observations of solitons in optical fibers [80]. Solitons emerge as fundamental solutions to the nonlinear Schrödinger equation because the dispersion term can balance the nonlinear term. In quantum optics the Gross-Pitaevskii equation is used to describe the evolution of the Bose-Einstein condensate ground state wave function.

The propagation constant can be achieved either from calculations or experimental investigations of the fiber and is often expressed in terms of a Taylor expansion

$$\beta(\omega) = \frac{n_{eff}(\omega)\omega}{c} = \sum_m \frac{1}{m!}\beta_m(\omega-\omega_0)^m; \beta_m = \frac{\partial^m \beta}{\partial \omega^m}\Big|_{\omega=\omega_0} \quad (12)$$

Any dispersion profile can be fitted with a Taylor polynomial, the question is only how many terms are needed to make a good fit over the width of the spectrum.

9. Calculation of the propagation

The linear part is

$$\frac{d^2}{dz^2}\tilde{G}(z,\omega) + \beta(\omega)^2\tilde{G}(z,\omega) = -\frac{\omega^2}{c^2}\frac{x^{(3)}}{A_{eff}(\omega)}\tilde{p}(z,\omega). \quad (13)$$

$$\frac{d^2}{dz^2}\hat{G}(z,\omega) = -\beta(\omega)^2\hat{G}(z,\omega), \quad (14)$$

and Eq. (6) both originate from Maxwell's linear equations. By considering the magnetic field $\mathbf{H}\omega(\mathbf{r})$ as given by Eq. (7) and taking the second derivative with respect to z the following equation arises

$$\frac{d^2}{dz^2}H_\omega(r) = -\beta(\omega)^2 H_\omega(r). \quad (15)$$

The magnetic and electric fields are related by

$$E_\omega(r) = -\frac{ic}{\omega\varepsilon(x,y)}\nabla \times H_\omega(r), \quad (16)$$

where with translational symmetry $\varepsilon(x, y)$ is independent of z. Consequently, $\mathbf{E}\omega(\mathbf{r})$ also fulfills Eq.(14) and $\beta(\omega)$ in this and the previous chapter is the same.

Nonlinear effects

As mentioned, Eq. (17)

$$\frac{d}{dz}\tilde{A}(\omega_1) = i(\beta(\omega)-\beta_1\omega)\tilde{A}(\omega_1) + i\gamma(\omega\int_{-\infty}^{\infty} dt e^{i\omega_1 t}A(t)\times\int_{-\infty}^{\infty} dt_1\ g(t-t_1)\,|\,A(t_1)\,|^2, \quad (17)$$

can be implemented directly as it is including both full frequency dependency of the propagation constant and the effective area as well as self-steepening and Raman effects.

Raman response

For the Raman response function the expression $g(t) = (1- fR)\delta(t) + f_R g_R(t)$ has been used, where the delta function term originates from the electronic response i.e. the Kerr interaction and the last term takes the Raman scattering into account. The function $g_R(t)$ can be chosen on the form

$$g_R(t) = \frac{\tau_1^2+\tau_2^2}{\tau_1\tau_2^2}e^{\frac{-t}{\tau_2}}\sin\left(\frac{t}{\tau_1}\right); t>0, \quad (18)$$

$$g_R(t) = 0; t<0, \quad (19)$$

as given by [81]. Raman scattering can be explained as scattering of light on the optical phonons and $1/\tau 1$ gives the optical phonon frequency. $1/\tau 2$ gives the bandwidth of the Lorentzian line (see **Fig.7**) . The same values as in [79] have been applied for the constants: $\tau 1 = 12.2fs$, $\tau 2 = 32fs$, $f_R = 0.18$.

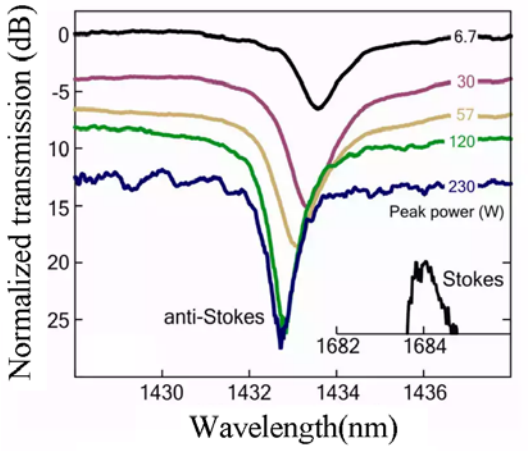

Fig. 7. Inverse Raman scattering are corollary processes arising in Raman scattering.

Kerr nonlinearity

The Kerr effect is the effect of an instantaneously occurring nonlinear response, which can be described as modifying the refractive index. In particular, the refractive index for the high intensity light beam itself is modified according to

$$\Delta n = n_2 \left| \right. \tag{20}$$

with the nonlinear index n_2 and the optical intensity I. The n_2 value of a medium can be measured e.g. with the z-scan technique. Note that in addition to the Kerr effect, electrostriction can significantly contribute to the value of the nonlinear index [82, 83]. A Kerr nonlinearity can be assumed by ignoring the Raman response in the fibers corresponding to setting $g(t) = \delta(t)$. If the nonlinearity factor is assumed constant $\gamma = \gamma 0$ the following equation arises

$$\frac{d}{dz}\tilde{A}(\omega_1) = i(\beta(\omega) - \beta_1)\tilde{A}(\omega_1) + i\gamma_0 \int_{-\infty}^{\infty} dt e^{i\omega_1 t} A(t)\left|A(t)\right|^2 . \tag{21}$$

If all terms are transformed to the time domain and only up to second order dispersion is taken into account the following equation appears

$$\frac{d}{dz}A(t) = -i\frac{\beta_2}{2}\frac{\partial^2}{\partial t^2}A(t) + i\gamma\left|A\right|^2 A(t) . \tag{22}$$

This is exactly the simple form of the nonlinear Schrödinger equation (11) .

Nonlinearity factor γ

For the nonlinearity factor the convention suggested in [79] has been followed

$$\gamma(\omega) = \frac{n_2\omega}{cA_{eff}(\omega)} . \tag{23}$$

The frequency dependent nonlinearity factor $\gamma(\omega)$ in Eq. (23) . Since the effective area $A_{\text{eff}}(\omega)$ often does not vary too drastically with frequency as seen on **Fig. 6** a valuable approximation is to assume the effective area to be constant $A_{\text{eff}},0$. With this approximation the nonlinearity factor can be written as

$$\gamma(\omega) = \frac{n_2 \omega}{c A_{eff,0}} = \gamma_0 \left(1 + \frac{\omega_1}{\omega_0} \right) \tag{24}$$

where $\omega_0 = \omega - \omega 1$ is the frequency of the input pulse and $\gamma_0 = \frac{n_2 \omega_0}{c A_{eff,0}}$. With this nonlinearity factor the nonlinear Schrödinger equation is given by

$$\frac{d}{dz} \tilde{A}(\omega_1) = i(\beta(\omega) - \beta_1 \omega) \tilde{A}(\omega_1) + i\gamma_0 \left(1 + \frac{\omega_1}{\omega_0} \right) \int_{-\infty}^{\infty} dt e^{i\omega_1 t} A(t) \int_{-\infty}^{\infty} dt_1 g(t - t_1) \left| A(t_1) \right|^2 . \tag{25}$$

In the time domain the nonlinearity factor above is given by $\gamma_0 \left(1 + i \frac{1}{\omega_0} \frac{\partial}{\partial t} \right)$, where the time derivative takes self-steepening and shock formation into account. Consequently, for very long pulses this time derivative can be omitted corresponding to assuming a constant nonlinearity factor

$$\gamma(\omega) = \gamma_0 . \tag{26}$$

If the computational grid is centered at a frequency ωc different from the central frequency of the pulse ω_0 the nonlinearity factor has to be changed accordingly $\gamma_0 = \frac{n_2 \omega_c}{c A_{eff,0}}$.

10. Conclusion

The transverse micro-structuring makes the dispersion of the fibers highly tunable and together with the high index contrast it leads to the small effective area, cade of nonlinear effects can take place in the fibers. The interplay between the special dispersion of the fibers and these nonlinear effects makes the phenomenon of supercontinuum generation possible. The linear Maxwell's equations have been solved for the transverse structure of the fibers. Starting with Maxwell's equations it has been sketched how a nonlinear Schrödinger equation for wave propagation in the PCFs can be achieved. The full frequency dependency of the propagation constant as well as the effective transverse area serve as input for the model and these parameters can either be calculated as measured. The model includes the instantaneous nonlinear response of silica. Additionally, the effects of Raman scattering, self steepening and shock formation can be included. In the following chapter most of the simulations shown will be based on Eq. (25) and the influence of the nonlinear effects will be investigated by comparison with the simpler version Eq. (21).

References

[1] *Rayleigh, J. W. S.* (1888). "On the remarkable phenomenon of crystalline reflexion described by Prof. Stokes," Phil. Mag, 26, 256–265.

[2] *Yablonovitch, E.* (1987). "Inhibited Spontaneous Emission in Solid-State Physics and Electronics," Phys. Rev. Lett, 58, 2059–2062.

[3] *Joannopoulos, J. et al.* (1995)."Photonic Crystals"*, Princeton Press, Princeton, N.J.*

[4] *Yablonovitch, E., Gmitter, T. J., Leung, K. M.* (1991). "Photonic Band Structure: The Face-Centered-Cubic Case Employing Nonspherical Atoms," Phys. Rev. Lett, 67, 2295-2298

[5] *Chan, C. T., Datta, S. Yu, Sigalas, Q. L., Ho, M., K. M. Soukoulis, C. M.* (1994)"New structures and algorithms for photonic band gaps," Physica A 211, 411–419.

[6] *Chan, C. T. Lu, Q. L., Ho, K. M.* (1995). "Order-N spectral method for electromagnetic waves," Phys. Rev. B 51, 16635–16642.

[7] *Fan, S., Villeneuve, P. R., Joannopoulos, J. D.* (1996). "Large omnidirectional band gaps in metallodielectric photonic crystals," Phys. Rev. B 54, 11245–11251.

[8] K. Sakoda, H. Shiroma, "Numerical method for localized defect modes in photonic lattices," Phys. Rev. B 56, 4830-4835 (1997)

[9] *Arriaga, J., Ward, A. J., Pendry, J. B.* (1999). "Order N photonic band structures for metals and other dispersive materials," Phys. Rev. B 59, 1874–1877.

[10] *Ward, A. J., Pendry, J. B.* (2000). "A program for calculating photonic band structures, Green's functions and transmission/reflection coefficients using a non-orthogonal FDTD method," Comput. Phys. Comm. 128, 590–621.

[11] *Pendry, J. B., MacKinnon, A.* (1992). "Calculation of photon dispersion relations," Phys. Rev. Lett. 69, 2772–2775.

[12] *Bell, P. M., Pendry, J. B., Moreno, L. M., Ward, A. J.* (1995)"A program for calculating photonic band structures and transmission coefficients of complex structures," Comput. Phys. Comm. 85, 306–322.

[13] *Elson, J. M., Tran, P.* (1996). "Coupled-mode calculation with the R-matrix propagator for the dispersion of surface waves on truncated photonic crystal," Phys. Rev. B 54, 1711–1715.

[14] *Chongjun, J., Bai, Q., Miao, Y., Ruhu, Q.* (1997). "Two-dimensional photonic band structure in the chiral medium-transfer matrix method," Opt. Commun, 142, 179–183.

[15] *Johnson, S. G., Joannopoulos, J. D.* (2001). "Block-iterative frequency-domain methods for Maxwell's equations in a planewave basis," Opt. Express 8, 173–190.

[16] *Danner, A. J., Raftery, Jr. J. J., Yokouchi, N., Choquette, K. D.* (2004). Transverse modes of photonic crystal vertical-cavity lasers. Appl. Phys. Lett, 84, 1031–1033.

[17] *Anderson, M., Ensher, J., Matthews, M., Wieman, C., Cornell, E.* (1995). Science 269, 198.

[18] *Davis, K., Mewes, M. O., Andrews, M., van Druten, N., Durfee, D., Kurn, D., Ketterle, W.* (1995).Phys. Rev. Lett. 75, 3969.

[19] *Russell, P. S. J.* (2003). "Photonic Crystal Fibres" Science 299, 358–362.

[20] *Russell, P. S. J.* (2006). J. Lightwave Technol. 24, 4729.

[21] *Knight, J. C., Broeng, J., Birks, T. A., Russell, P. S. J.* (1998). Science 282, 1476.

[22] *Konorov, S. O., Fedotov, A. B., Kolevatova, O. A., Beloglazov, V. I., Skibina, N. B., Shcherbakov, A. V., Zheltikov, A. M.* (2002). JETP Lett. 76, 341.

[23] *Litchinitser, N. M., Abeeluck, A. K., Headley, C., Eggleton, B. J.* (2002). Opt. Lett. 27, 1592.

[24] *Cregan, R. F., Mangan, B. J., Knight, J. C., Birks, T. A., Russell, P. S. J., Roberts, P. J., Allan, D. A.* (1999). Science 285, 1537.

[25] *Zheltikov, A. M.* (2004). Phys. Uspekhi 47, 1205.

[26] *Luan, F., George, A. K., Hedley, T. D., Pearce, G. J., Bird, D. M., Knight, J. C., Russell, P. S. J.* (2004). Opt. Lett. 29, 2369.

[27] *Marcatili, E. A. J., Schmeltzer, R. A.* (1964). Bell Syst. Tech. J. 43, 1783.

[28] Adams, M. J. (1981). An Introduction to Optical Waveguides, Wiley: New York.

[29] *Zheltikov, A. M.* (2004). Phys. Uspekhi 47, 69.

[30] *Knight, J. C., Birks, T. A., Russell, P. S. J., Atkin, D. M.* (1996). Opt. Lett. 21, 1547.

[31] *Ferrando, A., Silvestre, E., Miret, J. J., Andres, P.* (2000). Opt. Lett. 25, 790.

[32] *Reeves, W. H., Skryabin, D. V., Biancalana, F., Knight, J. C., Russell, P. S. J., Omenetto, F. G., Efimov, A., Taylor, A. J.* (2003). Nature 424, 511.

[33] *Fedotov, A. B., Zheltikov, A. M., Tarasevitch, A. P., von der Linde, D.* (2001). Appl. Phys. B 73, 181 (2001).

[34] *Ranka, J. K., Windeler, R. S., Stentz, A. J.* (2000). Opt. Lett. 25, 25.

[35] *Dudley, J. M., Genty, G., Coen, S.* (2006). Rev. Mod. Phys. 78, 1135.

[36] *Jones, D. J., Diddams, S. A., Ranka, J. K., Stentz, A.,Windeler, R. S., Hall, J. L., Cundiff, S. T.* (2000). Science 288, 635.

[37] *Udem, T., Holzwarth, R., Hänsch, T. W.* (2002). Nature 416, 233.

[38] *Serebryannikov, E. E., Zheltikov, A. M., Ishii, N., Teisset, C. Y., Köhler, S., Fuji, T., Metzger, T., Krausz, F., Baltuška, A.* (2005). Phys. Rev. E 72, 056603.

[39] *Teisset, C. Y., Ishii, N., Fuji, T., Metzger, T., Köhler, S., Holzwarth, R., Baltuska, A., Zheltikov, A. M., Krausz, F.* (2005). Opt. Express 13, 6550.

[40] *Hartl, I., Li, X. D., Chudoba, C., Rhanta, R. K., Ko, T. H., Fujimoto, J. G., Ranka, J. K., Windeler, R. S.* (2001). Opt. Lett. 26, 608.

[41] *Konorov, S. O., Akimov, D. A., Serebryannikov, E. E., Ivanov, A. A., Alfimov, M. V., Zheltikov, A. M.* (2004). Phys. Rev. E 70, 057601.

[42] *Zheltikov, A. M., Raman, J.* (2007). Spectrosc. 38, 1052.

[43] *Paulsen, H. N., Hilligsøe, K. M., Thøgersen, J., Keiding, S. R., Larsen, J. J.* (2003). Opt. Lett. 28, 1123.

[44] *Von Vacano, B., Wohlleben, W., Motzkus, M.* (2006). Opt. Lett. 31, 413.

[45] *Lim, H., Ilday, F.Ö., Wise, F.W.* (2002). Opt. Express 10, 1497.

[46] *Chen, X., Venkataraman, M., Li, N., Gallagher, M. T., Wood, W. A., Crowley, A. M., Carberry, J. P., Zenteno, L. A., Koch, K. W.* (2004). Opt. Express 12, 3888.

[47] *Lim, H., Chong, A., Wise, F. W.* (2005). Opt. Express, 13, 3460.

[48] *Isomäki, A., Khotnikov, O. G.* (2006). Opt. Express, 14, 4368.

[49] *Sharping, J. E., Fiorentino, M., Kumar, P., Windeler, R. S.* (2002). Opt. Lett, 27, 1675.

[50] *Deng, Y., Lin, Q., Lu, F., Agrawal, G. P., Knox, W. H.* (2005). Opt. Lett, 30, 1234.

[51] *Sharping, J. E., Chen, J., Li, X., Kumar, P., Windeler, R. S.* (2004).Opt. Express, 12, 3086.

[52] *Rarity, J. G., Fulconis, J., Duligall, J., Wadsworth, W. J., Russell, P. S. J.* (2005). Opt. Express, 13, 534.

[53] *Birks, T. A., Knight, J. C., Russell, P. S. J.* (1997). Opt. Lett, 22, 961.

[54] *Knight, J. C., Birks, T. A., Cregan, R. F., Russell, P. S. J., de Sandro, J. P.* (1998). Electron. Lett, 34, 1347.

[55] *Furusawa, K., Malinowski, A., Price, J., Monro, T., Sahu, J., Nilsson, J., Richardson, D.* (2001). Opt. Express 9, 714.

[56] *Wadsworth, W. J., Knight, J. C., Reeves, W. H., Russell, P. S. J.* (2000). Electron. Lett. 36, 1452.

[57] *Furusawa, K., Monro, T. M., Petropoulos, P., Richardson, D. J.* (2001). Electron. Lett. 37, 560.

[58] *Wadsworth, W., Percival, R., Bouwmans, G., Knight, J., Russell, P.* (2003). Opt. Express 11, 48.

[59] *Limpert, J., Schreiber, T., Nolte, S., Zellmer, H., Tünnermann, T., Iliew, R., Lederer, F., Broeng, J., Vienne, G., Petersson, A., Jakobsen, C.* (2003). Opt. Express 11, 818.

[60] *Südmeyer, T., Brunner, F., Innerhofer, E., Paschotta, R., Furusawa, K., Baggett, J. C., Monro, T. M., Richardson, D. J., Keller, U.* (2003). Opt. Lett. 28, 1951.

[61] *Mitrofanov, A. V., Ivanov, A. A., Alfimov, M. V., Podshivalov, A. A., Zheltikov, A. M.* (2007). Opt. Commun. 280, 453.

[62] *Mitrokhin, V. P., Ivanov, A. A., Fedotov, A. B., Alfimov, M. V., Dukel'skii, K. V., Khokhlov, A. V., Shevandin, V. S., Kondrat'ev, Yu. N., Podshivalov, A. A., Zheltikov, A. M.* (2007). Laser Phys. Lett. 4, 529.

[63] *Pickrell, G., Peng, W., Wang, A.* (2004). Opt. Lett. 29, 1476.

[64] *Konorov, S. O., Zheltikov, A. M., Scalora, M.* (2005). Opt. Express 13, 3454.

[65] *Jensen, J. B., Pedersen, L. H., Hoiby, P. E., Nielsen, L. B., Hansen, T. P., Folkenberg, J. R., Riishede, J., Noordegraaf, D., Nielsen, K., Carlsen, A., Bjarklev, A.* (2004). Opt. Lett. 29, 1974.

[66] *Limpert, J., Schreiber, T., Nolte, S., Zellmer, H., Tünnermann, A.* (2003). Opt. Express 11, 3332.

[67] *de Matos, C. J. S., Popov, S. V., Rulkov, A. B., Taylor, J. R., Broeng, J., Hansen, T. P., Gapontsev, V. P.* (2004). Phys. Rev. Lett. 93, 103901.

[68] *Bjarklev, A., Broeng, J., Bjarklev, A. S.* (2003). *Photonic crystal fibres* (Kluwer Academic Publishers, Boston).

[69] *Knight, J. C., Birks, T. A., Russell, P. S. J., de Sandro, J. P. Opt. J.* (1998). Soc. Am. A. 15, 748.

[70] *Birks, T. A., Knight, J. C., Russell, P. S. J.* (1997). Opt. Lett. 22, 961.

[71] *Kumar, V. V. R., George, A., Reeves, W., Knight, J., Russell, P., Omenetto, F., Taylor, A.* (2002). Extruded soft glass photonic crystal fiber for ultrabroad supercontinuum generation. Optics Express, 10 (25), 1520. doi: 10.1364/oe.10.001520

[72] *Cregan, R. F., Mangan, B. J., Knight, J. C., Birks, P. T. A., Russell, St. J., Roberts, P. J., Allan, D. C.* (1999). "Singlemode photonic band gap guidance of light in air," Science 285, 1537–1539.

[73] *Payne, F. P., Lacey, J. P. R.* (1994). "A theoretical analysis of scattering loss from planar optical waveguides," Opt. Quantum Electron. 26, 977-986.

[74] *Joannopoulos, J. D., Meade, R. D., Winn, J. N.* (1995). Photonic crystals – molding the flow of light (Princeton University Press), 1st ed.

[75] *Sakoda, K.* (2001). *Optical properties of photonic crystals* (Springer, Berlin), 1st ed.

[76] *Johnson, S. G., Joannopoulos, J. D.* (2001). Opt. Express 8, 173, URL http://www.opticsexpress.org/abstract.cfm?URI= OPEX-8-3-173.

[77] *Johnson, S. G., Joannopoulos, J. D.* (http://ab-initio.mit.edu/mpb/).

[78] *Mortensen, N. A.* (2002). Opt. Express 10, 341, URL http://www. opticsexpress.org/abstract.cfm?URI=OPEX-10-7-341.

[79] *Agrawal, G. P.* (2001). Nonlinear Fiber Optics (Academic Press), 3rd ed.

[80] *Mollenauer, L. F., Stolen, R. H., Islam, M. N.* (1980).Phys. Rev. Lett. 45, 1095.

[81] *Blow, K. J., Wood, D., IEEE J.* (1989). Quantum Electron. 25, 2665.

[82] *Buckland, E. L., Boyd, R. W.* (1996). "Electrostrictive contribution to the intensity-dependent refractive index of optical fibers", Opt. Lett. 21 (15), 1117.

[83] *Buckland, E. L., Boyd, R. W.* (1997). "Measurement of the frequency response of the electrostrictive nonlinearity in optical fibers", Opt. Lett. 22 (10), 676.